Eur. Phys. J. C (2020) 80:521
https://doi.org/10.1140/epjc/s10052-020-8095-3

THE EUROPEAN PHYSICAL JOURNAL C

Regular Article - Theoretical Physics

Single inclusive jet photoproduction at very forward rapidities in pp and pPb collisions at the LHC

V. P. Gonçalves[a] **, G. Sampaio dos Santos, C. R. Sena**

High and Medium Energy Group, Instituto de Física e Matemática, Universidade Federal de Pelotas, Caixa Postal 354, Pelotas, RS 96010-900, Brazil

Received: 10 May 2020 / Accepted: 27 May 2020 / Published online: 11 June 2020

Abstract The particle production at very forward rapidities is expected to be sensitive to the non-linear effects in the QCD dynamics at high energies. In this paper we present, for the first time, the predictions of the Color Dipole formalism for the single inclusive jet photoproduction in pp and pPb collisions considering the very forward rapidities probed by the CMS-CASTOR calorimeter, which will be characterized by a jet in the rapidity range of $5.2 \leq Y \leq 6.6$, a rapidity gap in the rapidity range probed by the central CMS detector and one of the incident hadrons remaining intact in the final state. The transverse momentum distributions and energy spectra are estimated considering the more recent phenomenological models for the dipole-proton scattering amplitude, which are based on the Color Glass Condensate formalism and are able to describe the inclusive and exclusive ep HERA data. Our results indicate that a future experimental analysis of this process is, in principle, feasible and useful to constrain the description of the QCD dynamics at high energies.

1 Introduction

The partonic structure of the hadrons at high energies is determined by the gluon distribution at small values of the Bjorken-x variable, which is predicted by the linear DGLAP equation to increase with the energy [1–3]. Such behavior implies that the hadrons become a dense system and that for a given scale, denoted saturation scale $Q_s(x)$, the non-linear effects, disregarded by the DGLAP equation, should be taken into account [4]. During the last years, our knowledge about the QCD dynamics at high energies have had a substantial development [5–7]. However, several open questions still remain, which implies that the underlying assumptions of the different approaches should still be tested by the comparison of its predictions with the future experimental data for high energy processes [8–12].

The description of the QCD dynamics in hadronic colliders is expected to be more easily constrained in the particle production at forward rapidities, where the wave function of one of the projectiles is probed at large Bjorken-x and that of the other at very small x (For a review see, e.g. Ref. [13]). The latter is characterized by a large number of gluons, which is expected to form a new state of matter - the Color Glass Condensate (CGC) - where the gluon distribution saturates and non-linear coherence phenomena dominate [5–7]. The main features of particle production are determined by the saturation scale, whose evolution is described by an infinite hierarchy of coupled equations for the correlators of Wilson lines [14–26]. In this regime, the partons of the projectile undergoes multiple scatterings, which cannot be encoded in the traditional (collinear and k_T) factorization schemes. During the last years, several authors have discussed the forward particle production in hadronic collisions using the hybrid approach, which takes into account of the factorization breaking effects as well as of the non-linear corrections to the QCD dynamics, with the predictions being compatible with the RHIC and LHC data (See, e.g. Refs. [27–29]). In particular, in Refs. [30–32] the authors have presented its predictions for the single inclusive jet transverse momentum spectrum at very forward rapidity ($5.2 \leq Y \leq 6.6$) in pp and pPb collisions, which is ideal to probe the non-linear effects and corresponds to the acceptance of the CMS-CASTOR calorimeter, which is installed on one side of the nominal interaction point of the CMS experiment. These results indicated that the transverse momentum and energy spectra are sensitive to the non-linear effects. In Ref. [32] the authors have demonstrated that the jet-energy spectra computed in the CGC formalism are compatible with the measurements performed by the CMS-CASTOR calorimeter, which were recently published [33]. Our focus in this paper is not in the single jet production analyzed in the recent CMS-CASTOR

[a] e-mail: barros@ufpel.edu.br (corresponding author)

study, where the events are characterized by the dissociation of both incident hadrons, but instead in the proposition of an alternative process that allow us to probe the QCD dynamics at very small-x and can be analyzed using the CMS-CASTOR calorimeter in conjuction with the central CMS detector and the CMS-TOTEM precision proton spectrometer (CT-PPS). We propose the study of the single inclusive jet photoproduction at very forward rapidities in ultraperipheral pp and pPb collisions. Such process is present in photon-induced interactions, which are dominant when the impact parameter of the collision is larger than the sum of the radius of the incident hadrons [34–41], and is characterized by one rapidity gap (associated to the photon exchange), with the incident hadron that emits the photon remaining intact in the final state. A typical diagram is presented in Fig. 1. In principle, the intact hadron can be tagged by the CT-PPS and the rapidity gap observed by the central CMS detector, with the jet being produced in the kinematical rapidity range probed by the CMS-CASTOR calorimeter. Such topology strongly reduces the background associated to inclusive hadronic collisions, where both incident hadrons fragment. In addition, the contribution of single diffractive interactions, mediated by a Pomeron exchange, which can generate a similar topology, are subleading in pPb collisions and can be suppressed in pp collisions by imposing a cut in the transverse momentum of the intact hadron (For a detailed discussion see, e.g. [42]). In this paper we will estimate, for the first time, the transverse momentum distribution and energy spectra for the single inclusive jet photoproduction in pp collisions at $\sqrt{s} = 13$ TeV and pPb collisions at $\sqrt{s} = 5.02$ TeV considering that the jet J is produced in the rapidity region of $5.2 \leq Y \leq 6.6$. Using the Color Dipole formalism [43,44], we will express the single jet photoproduction cross section in terms of the dipole-target scattering amplitude, which is determined by the QCD dynamics at high energies. In our analysis, the transverse momentum distributions will be estimated considering the more recent phenomenological models for the dipole-proton scattering amplitude, which are based on the Color Glass Condensate formalism and are able to describe the inclusive and exclusive ep HERA data. As a consequence, our predictions for the single jet photoproduction cross sections at the LHC are parameter free. As we will demonstrate below, a future experimental analysis of this process can be useful to constrain the description of the QCD dynamics at high energies.

This paper is organized as follows. In the next section we will present a brief review of the Color Dipole formalism for the single jet photoproduction in hadronic collisions. In Sect. 3 we present our predictions for the transverse momentum distributions and energy spectra of the single jet photoproduction in the rapidity range probed by the CMS-CASTOR calorimeter considering pp collisions at $\sqrt{s} = 13$ TeV and pPb collisions at $\sqrt{s} = 5.02$ TeV. Finally, in Sect. 4 we summarize our main conclusions.

2 Single jet photoproduction in hadronic collisions

The study of photon-interactions in hadronic collisions became a reality in the last years [34–41], strongly motivated by the possibility of constrain the description of the QCD dynamics at high energies [45,46]. One of the more studied processes is the exclusive vector meson photoproduction in $pp/pPb/PbPb$ collisions [45–79], where both incident hadrons remain intact and two rapidity gaps are present in the final state, with the basic motivation been associated to the fact that its cross section is proportional to the square of the gluon distribution (in the collinear formalism) [45]. Another possibility, is to probe the QCD dynamics in photon-induced interactions where one the incident hadrons break up and only one rapidity gap is present in the final state, usually denoted inclusive processes. Examples of inclusive

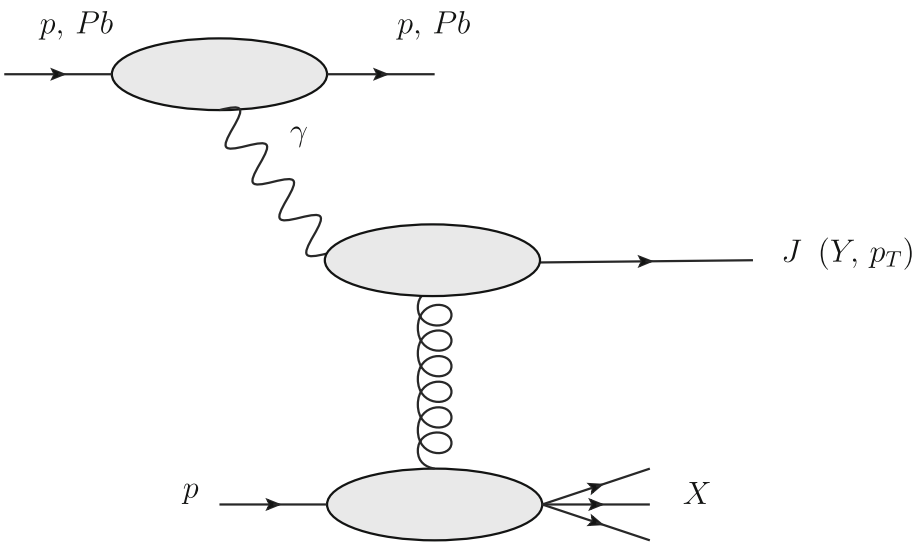

Fig. 1 Typical diagram for the single inclusive jet photoproduction in a hadronic collision

processes are the heavy quark and dijet photoproduction in hadronic collisions [42,81–93]. In contrast to the exclusive processes, in the inclusive case we have that: (a) the cross sections are proportional to the first power of the gluon distribution (in the collinear formalism), and (b) the experimental separation becomes harder in comparison to the exclusive one. However, its cross sections are in general one order of magnitude larger. The recent results obtained by the ATLAS Collaboration [94], indicated that its experimental separation is, in principle, feasible. Such aspects motivate the analysis of the single inclusive jet photoproduction in ultraperipheral pp/pPb collisions at the LHC energies.

In an ultraperipheral hadronic collision, the impact parameter is such that $b > R_1 + R_2$, where R_i is the radius of the hadron i, which implies that the photon-induced interactions become dominant. In this regime, the ultrarelativistic hadrons act as a source of almost real photons and the hadron-hadron cross section can be written in a factorized form, described using the equivalent photon approximation [34–41,95]. As a consequence, the differential cross section for the photoproduction of a single jet J with transverse momentum p_T at rapidity Y in a hadronic collision, represented in Fig. 1, is given by

$$\frac{d^2\sigma\ [h_1 + h_2 \to h_i + J + X]}{dY d^2p_T} = \left[n_{h_1}(\omega)\, \frac{d\sigma_{\gamma h_2 \to JX}}{d^2p_T}\left(W^2_{\gamma h_2}\right)\right]_{\omega=\omega_L} + \left[n_{h_2}(\omega)\, \frac{d\sigma_{\gamma h_1 \to JX}}{d^2p_T}\left(W^2_{\gamma h_1}\right)\right]_{\omega=\omega_R}, \quad (1)$$

where h_i denotes the hadron that acted as the source of photons and will remain intact in the final state, and ω_L ($\propto e^{+Y}$) and ω_R ($\propto e^{-Y}$) denote photons from the h_1 and h_2 hadrons, respectively. Moreover, $n(\omega)$ is the equivalent photon spectrum generated by the hadronic source and $d\sigma/d^2p_T$ is the differential cross section for the single jet photoproduction in a photon-hadron interaction with center-of-mass energy $W_{\gamma h} = \sqrt{4\omega E}$, where $E = \sqrt{s}/2$ and $\sqrt{s}$ is the hadron-hadron c.m. energy. The final state will be characterized by one rapidity gap, associated to the photon exchange, and an intact hadron in the final state, which was the photon source. As in our previous studies [76–78], we will assume that the photon flux associated to the proton and nucleus can be described by the Drees-Zeppenfeld [96] and the relativistic point-like charge [34–41] models, respectively. The single jet quark photoproduction cross section will be estimated using the Color Dipole formalism [43,44], which provides a unified description of inclusive and exclusive ep observables and allows to describe the γh interaction in terms of a (color) dipole-hadron interaction, which is directly associated to the description of the QCD dynamics at high energies. As demonstrated in detail e.g. in Ref. [97], the cross section for the single jet photoproduction can be expressed in terms of the photon wave function Ψ, which describes the photon fluctuation into a color dipole which interacts with the target via strong interaction, with this interaction being described by the dipole-hadron cross section σ_{dh}. In particular, the transverse momentum distribution of a single jet J with momentum p_T will be given by [97,98]

$$\frac{d\sigma(\gamma h \to JX)}{d^2p_T} = \frac{1}{(2\pi)^2}\sum_f \int d^2\mathbf{r_1}\, d^2\mathbf{r_2}\, d\alpha\, e^{i\mathbf{p_T}\cdot(\mathbf{r_1}-\mathbf{r_2})} \times \left[\Psi^T(\alpha,\mathbf{r_1})\Psi^{*T}(\alpha,\mathbf{r_2})\right]_f \times \frac{1}{2}\left\{\sigma_{dh}(x,\mathbf{r_1}) + \sigma_{dh}(x,\mathbf{r_2}) - \sigma_{dh}(x,\mathbf{r_1}-\mathbf{r_2})\right\}, \quad (2)$$

where α is the photon momentum fraction carried by the quark and $\mathbf{r_1}$ and $\mathbf{r_2}$ are the transverse dipole separations in the amplitude and its complex conjugate, respectively. As shown in Refs. [97,98], for a transversely polarized photon with $Q^2 = 0$ one has that the overlap function $\left[\Psi^T(\alpha,\mathbf{r_1})\Psi^{*T}(\alpha,\mathbf{r_2})\right]_f$ for a given flavour f ($= u, d, s, c$ and b) is given by

$$\left[\Psi^T(\alpha,\mathbf{r_1})\Psi^{*T}(\alpha,\mathbf{r_2})\right]_f = \frac{6\,\alpha_{em}\,e_f^2}{(2\pi)^2}\left\{m_f^2 K_0(m_f r_1)K_0(m_f r_2) + m_f^2\left[\alpha^2+(1-\alpha)^2\right]\frac{\mathbf{r_1}\cdot\mathbf{r_2}}{r_1 r_2}K_1(m_f r_1)K_1(m_f r_2)\right\}, \quad (3)$$

where e_f is the fractional quark charge and m_f the mass of the quark. Moreover, the dipole-hadron cross section, σ_{dh}, can be expressed by

$$\sigma_{dh}(x,r^2) = 2\int d^2\boldsymbol{b}_h\, \mathcal{N}^h(x,\boldsymbol{r},\boldsymbol{b}_h), \quad (4)$$

where $\boldsymbol{b}_h$ is the impact parameter, given by the transverse distance between the dipole center and the target center, and $\mathcal{N}^h(x,\boldsymbol{r},\boldsymbol{b}_h)$ is the forward dipole-hadron scattering amplitude, which is dependent on the modelling of the QCD dynamics at high energies (See below). Furthermore, the Bjorken-x variable is given by $x = (4m_f^2 + p_T^2)/W^2_{\gamma h}$. As the photon energy ω_L increases with the rapidity and $W_{\gamma h} \propto (\omega)^{1/2}$, we have that the single jet photoproduction for the rapidities probed by the CMS-CASTOR calorimeter will be strongly dependent of the treatment of the QCD dynamics for very small values of x ($\leq 10^{-5}$). The Eq. (2) can be reexpressed as follows [98]

$$\frac{d\sigma(\gamma h \to JX)}{d^2p_T} = \frac{6\,e_f^2\,\alpha_{em}}{(2\pi)^2}\int d\alpha\left\{m_f^2\left[\frac{I_1}{p_T^2+m_f^2} - \frac{I_2}{4\,m_f}\right] + \left[\alpha^2+(1-\alpha)^2\right]\left[\frac{p_T\,m_f\,I_3}{p_T^2+m_f^2} - \frac{I_1}{2} + \frac{m_f\,I_2}{4}\right]\right\}, \quad (5)$$

where the quantities I_i are auxiliary functions defined in terms of integrals over the dipole size r of the dipole-hadron

cross section and combinations of Bessel functions:

$$I_1 = \int dr\, r\, J_0(p_T\, r)\, K_0(m_f\, r)\, \sigma_{dh}(r) \tag{6}$$

$$I_2 = \int dr\, r^2\, J_0(p_T\, r)\, K_1(m_f\, r)\, \sigma_{dh}(r) \tag{7}$$

$$I_3 = \int dr\, r\, J_1(p_T r)\, K_1(m_f\, r)\, \sigma_{dh}(r)\ , \tag{8}$$

with the functions $K_{0,1}$ ($J_{0,1}$) being the modified Bessel functions of the second (first) kind.

The main ingredient for the calculation of the transverse momentum spectrum is the dipole-hadron cross section, which is determined by the dipole-target scattering amplitude $\mathcal{N}_h$. The treatment of this quantity is a subject of intense study by several groups [5–7]. During the last decades, several phenomenological models based on the Color Glass Condensate formalism [5–7] have been proposed to describe the HERA data taking into account the non-linear effects in the QCD dynamics. In general, such models differ in the treatment of the impact parameter dependence and/or of the linear and non-linear regimes. Currently, the bCGC and IP-SAT models, which are based on different assumptions for the treatment of the gluon saturation effects, describe with success the high precision HERA data for inclusive and exclusive ep processes. The diagramatic representation of the saturation effects included in the IP-SAT and bCGC models for the description of the dipole-hadron scattering amplitude at high energies is presented in Fig. 2a and b, respectively. In the impact parameter Color Glass Condensate (bCGC) model [99] the dipole-proton scattering amplitude is given by

$$\mathcal{N}^p(x, \boldsymbol{r}, \boldsymbol{b}_p) = \begin{cases} \mathcal{N}_0 \left(\frac{r\, Q_s(b_p)}{2}\right)^{2\left(\gamma_s + \frac{\ln(2/r\, Q_s(b_p))}{\kappa\, \lambda\, y}\right)} & r\, Q_s(b_p) \leq 2 \\ 1 - e^{-A\, \ln^2\,(B\, r\, Q_s(b_p))} & r\, Q_s(b_p) > 2, \end{cases} \tag{9}$$

with $\kappa = \chi''(\gamma_s)/\chi'(\gamma_s)$, where χ is the LO BFKL characteristic function and $y = \ln(1/x)$. The coefficients A and B are determined uniquely from the condition that $\mathcal{N}^p(x, \boldsymbol{r}, \boldsymbol{b}_p)$, and its derivative with respect to $r\, Q_s(b_p)$, are continuous at $r\, Q_s(b_p) = 2$. The impact parameter dependence of the proton saturation scale $Q_s(b_p)$ is given by:

$$Q_s(b_p) \equiv Q_s(x, b_p) = \left(\frac{x_0}{x}\right)^{\frac{\lambda}{2}} \left[\exp\left(-\frac{{b_p}^2}{2B_{\rm CGC}}\right)\right]^{\frac{1}{2\gamma_s}}, \tag{10}$$

with the parameter $B_{\rm CGC}$ being obtained by a fit of the t-dependence of exclusive J/ψ photoproduction. The factors $\mathcal{N}_0$ and γ_s were taken to be free. In what follows we consider the set of parameters obtained in Ref. [100] by fitting the recent HERA data on the reduced ep cross sections: $\gamma_s = 0.6599$, $\kappa = 9.9$, $B_{CGC} = 5.5\ \text{GeV}^{-2}$, $\mathcal{N}_0 = 0.3358$, $x_0 = 0.00105$ and $\lambda = 0.2063$. In the bCGC model, the saturation regime, where $r\, Q_s(b_p) > 2$, is described by the Levin-Tuchin law [101] and the linear one by the BFKL dynamics near of the saturation line. On the other hand, in the IP-SAT model [102,103], $\mathcal{N}^p$ has an eikonalized form and depends on a gluon distribution evolved via DGLAP equation, being given by

$$\mathcal{N}^p(x, \boldsymbol{r}, \boldsymbol{b}_p) = 1 - \exp\left[-\frac{\pi^2 r^2}{2N_c}\alpha_s(\mu^2)\ xg\left(x, \frac{C}{r^2} + \mu_0^2\right)\ T_G(b_p)\right], \tag{11}$$

with a Gaussian profile

$$T_G(b_p) = \frac{1}{2\pi\, B_G} \exp\left(-\frac{b_p^2}{2B_G}\right). \tag{12}$$

The initial gluon distribution evaluated at μ_0^2 is taken to be $xg(x, \mu_0^2) = A_g x^{-\lambda_g}(1-x)^6$. In this work we assume the parameters obtained in Ref. [104]. As in the bCGC model, the IP-SAT predicts the saturation of $\mathcal{N}^p$ at high energies and/or large dipoles, but the approach to this regime is not described by the Levin-Tuchin law. Moreover, in contrast to the bCGC model, the IP-SAT takes into account the effects associated to the DGLAP evolution, which are expected to be important in the description of small dipoles. Consequently, both models are based on different assumptions for the linear and non-linear regimes. As pointed above, the current high precision HERA data are not able to discriminate between these models. As we will demonstrate below, a future experimental analysis of the single jet photoproduction at the LHC can be useful to achieve this goal. In order to quantify the impact of the non-linear effects, we also will present the predictions derived neglecting the non- linear corrections, with the dipole-proton scattering amplitude being given by the linear part of the IP-SAT model, denoted hereafter IP-NONSAT, which is

$$\mathcal{N}^p(x, \boldsymbol{r}, \boldsymbol{b}_p) = \frac{\pi^2 r^2}{2N_c}\alpha_s(\mu^2)\ xg\left(x, \frac{C}{r^2} + \mu_0^2\right)\ T_G(b_p), \tag{13}$$

with the parameters obtained in Ref. [104].

In Fig. 3 we present a comparison between the IP-SAT, bCGC and IP-NONSAT predictions for the dipole-proton scattering amplitude as a function of r^2 for two different values of the variable x and considering central collisions ($b_p = 0$). We have that the description of the linear regime (small-r^2) is distinct in the bCGC and IP-SAT models, as well the transition between the linear and non – linear regimes, with the onset of the saturation regime ($\mathcal{N}^p \approx 1$) being slower in the case of the bCGC model. For small dipole sizes and $x = 10^{-3}$, we can observe the different r^2 dependence of the distinct models. In this regime, the bCGC model predicts

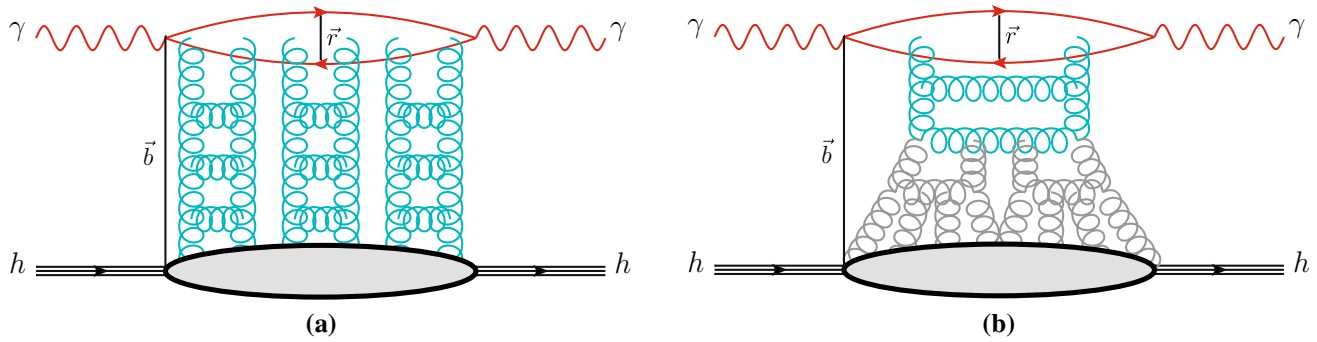

Fig. 2 Diagramatic representation of the saturation effects included in the **a** IP-SAT and **b** bCGC models for the description of the dipole-hadron scattering amplitude at high energies

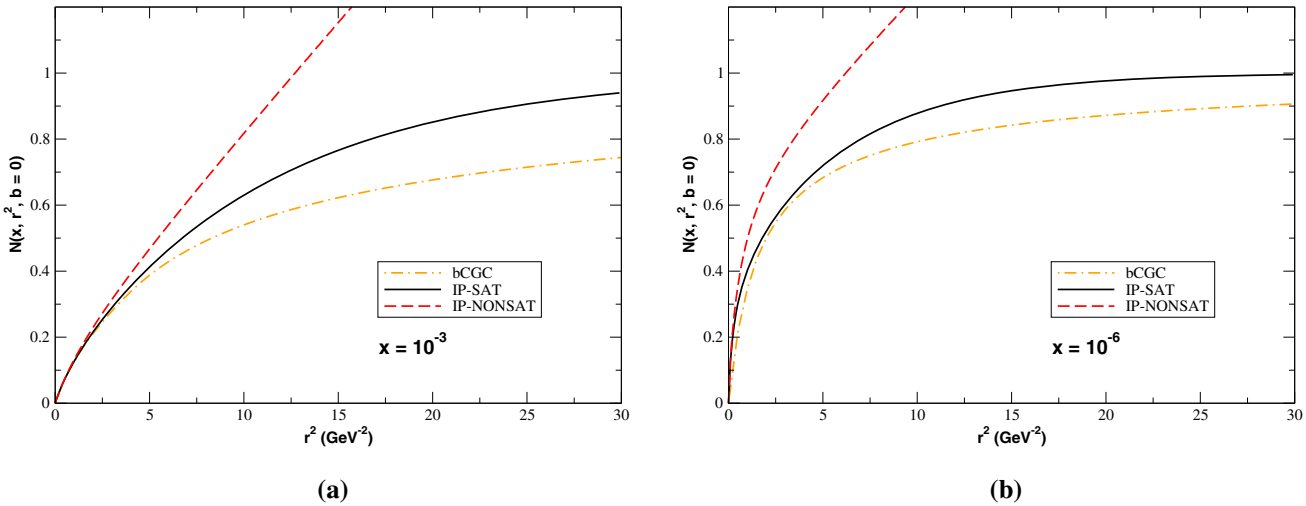

Fig. 3 Dipole-proton scattering amplitude as a function of the squared dipole size for two distinct values of x

that $\mathcal{N}^p \propto \boldsymbol{r}^{2\gamma_{eff}}$ for $r^2 \to 0$, while the IP-SAT and IP-NONSAT models predict that $\mathcal{N}^p \propto \boldsymbol{r}^2\, xg(x, 4/r^2)$. On the other hand, for large dipole sizes, the IP-SAT amplitude have a asymptotic value larger than the bCGC one. For $x = 10^{-6}$ we have that the onset of the saturation occurs at smaller values of r^2. The main difference between the bCGC and IP-SAT models is associated to the behavior predicted for the transition between the linear (small-r^2) and non-linear (large-r^2) regimes of the QCD dynamics. Since the single inclusive jet photoproduction cross section for different values of p_T probe distinct values of r, their analysis can be useful to discriminate between the different models for the dipole-proton scattering amplitude.

3 Results

In what follows we will present our predictions for the transverse momentum distribution and energy spectrum of the single inclusive jet photoproduction, integrated over the kinematical rapidity range of the CMS-CASTOR calorimeter ($5.2 \leq Y \leq 6.6$), considering pp collisions at $\sqrt{s} = 13$ TeV and pPb collisions at $\sqrt{s} = 5.02$ TeV. In the case of pPb collisions, we have verified that the transverse momentum spectrum is dominated by photon-proton interactions, with the photons generated by the nucleus. Such result is expected, due to the Z^2 enhancement present in the nuclear photon flux. Therefore, our predictions are only dependent on the model used for the dipole-proton scattering amplitude. As this quantity have been constrained by the HERA data in the case of the IP-SAT, IP-NONSAT and bCGC models, our predictions for the single jet photoproduction at the LHC are parameter free.

In Fig. 4a we present our predictions for the transverse momentum distribution considering pp collisions at $\sqrt{s} = 13$ TeV and the distinct dipole models discussed in the previous section. As expected, the IP-NONSAT model predicts larger values for the distribution in comparison to the IP-SAT prediction. We can also observe that the predictions of the IP-SAT and bCGC models differ at small and large values of

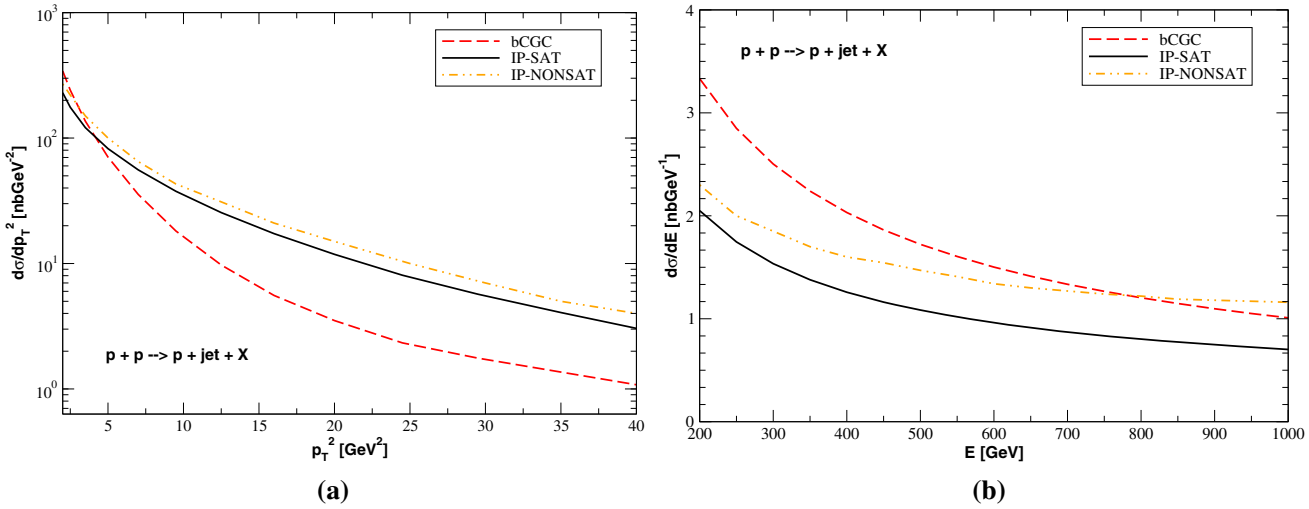

Fig. 4 Predictions for the **a** transverse momentum distribution and **b** energy spectrum for the single inclusive jet photoproduction at very forward rapidties in pp collisions at $\sqrt{s} = 13$ TeV

p_T^2. This difference is directly associated to the distinct treatments for the linear and non-linear regimes present in the IP-SAT and bCGC models. As discussed before, although the IP-SAT predicts the saturation of $\mathcal{N}^p$ at high energies (small values of x), the approach to this regime is not described by the Levin-Tuchin law, as in the bCGC model. We have that the distinct models predict a similar value of the distribution for $p_T^2 \approx 4\,\text{GeV}^2$, but the predictions are distinct at larger values of p_T^2. In this transverse momentum range, we are probing the transition between the linear and non-linear regimes, which are treated differently in the IP-SAT and bCGC models (See Fig. 3). Such distinct transition implies the difference observed in the figure. Moreover, our results indicate that the bGCG result becomes larger than the IP-SAT and IP-NONSAT predictions at small values of p_T^2. Finally, the results presented in Fig. 4a also indicate that the analysis of the transverse momentum distribution in the range $10 \lesssim p_T^2 \lesssim 40\,\text{GeV}^2$ can be useful to discriminate between the IP-SAT and bCGC predictions.

Using our results for the transverse momentum distribution, we can estimate the energy spectrum $d\sigma/dE$, which is the main observable measured by the CASTOR calorimeter at CMS. We have that [30]

$$\frac{d\sigma\left[h_1 + h_2 \to h_i + J + X\right]}{dE} = \int_{Y_{min}}^{Y_{max}} dY \frac{d\sigma}{dY d^2p_T} \frac{1}{\cosh Y}, \tag{14}$$

where we take $Y_{min} = 5.2$ and $Y_{max} = 6.6$, which corresponds to the CASTOR acceptance. The associated predictions for the energy spectrum considering the distinct dipole models are presented in Fig. 4b. In agreement with the results observed for the transverse momentum distribution, we have that the IP-NONSAT prediction is larger than the IP-SAT one. Moreover, we can observe that the bCGC model predicts a larger value for the energy spectrum for $E \leq 800$ GeV, which is associated to the fact that the spectrum is strongly dependent on the transverse momentum distribution at small p_T^2. We have verified that for $E > 2000$ GeV, the bCGC prediction becomes smaller than the IP-SAT one.

In Fig. 5a and b we present our predictions for the transverse momentum distribution and energy spectrum, respectively, considering pPb collisions at $\sqrt{s} = 5.02$ TeV. As discussed before, in this case the transverse momentum distribution is dominated by photon-proton interactions. As a consequence, in contrast to pp collisions, where both protons act as sources of photons, and the distribution for a given rapidity receives contributions of small and large energies, one has that the single jet photoproduction at very forward rapidities in pPb collisions is determined, in a very good approximation, only by the QCD dynamics at high energies. In addition, in comparison to the pp case, the cross sections for pPb collisions are larger by a factor $\approx 10^3$ due to the Z^2 enhancement in the nuclear photon flux. Regarding the transverse momentum distribution, presented in Fig. 5a, we can see that the p_T^2 dependence of the predictions are similar to those observed in Fig. 4a. As in the pp case, we propose the analysis of the transverse momentum distribution in the range $10 \lesssim p_T^2 \lesssim 40\,\text{GeV}^2$ to discriminate between the IP-SAT and bCGC predictions. The predictions for the energy spectrum are presented in Fig. 5b and indicated that this observable can be used to discriminate between the distinct dipole models. Our results indicate that a future experimental analysis of this final state can be useful to probe the Color Dipole formalism and the underlying assumptions present in the phenomenological saturation models.

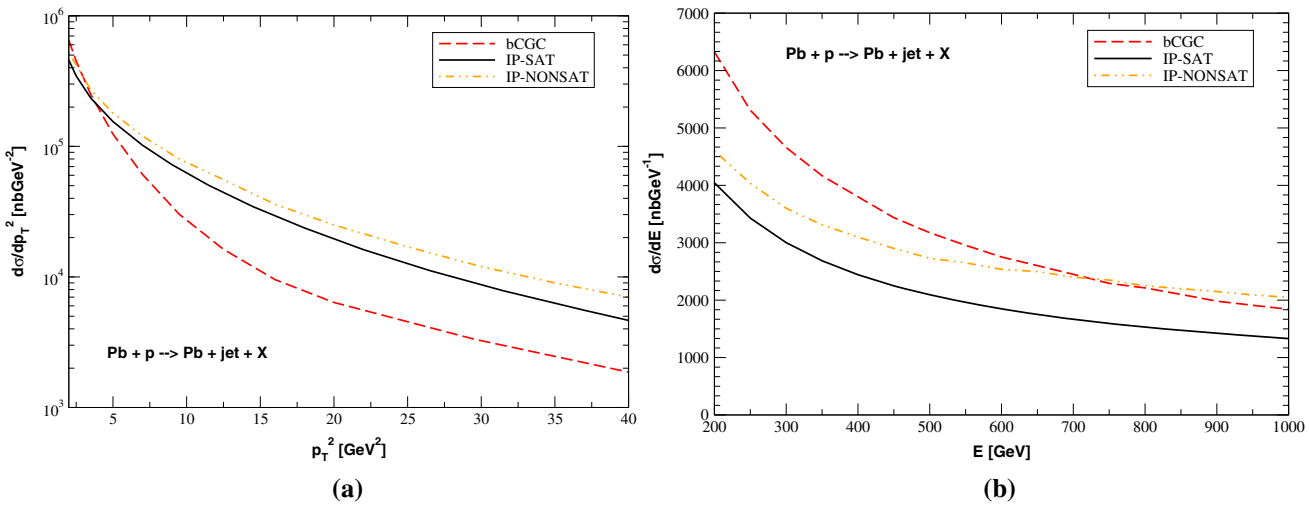

Fig. 5 Predictions for the **a** transverse momentum distribution and **b** energy spectrum for the single inclusive jet photoproduction at very forward rapidties in pPb collisions at $\sqrt{s} = 5.02$ TeV

4 Summary

The Large Hadron Collider (LHC) has opened up a new frontier in high energy hadron-hadron collisions, allowing to test the Quantum Chromodynamics in unexplored regimes of energy, density and rapidities, considering different configurations of the colliding hadrons (protons and nuclei). In particular, the LHC experiments have unprecedented capacities to study several subjects associated to Forward Physics and photon-induced interactions which allows to probe the description of the QCD dynamics at very small values of the Bjorken-x variable. In particular, the recent results for photon-induced interactions in hadronic colliders has indicated that the analysis of these processes can be useful to improve our understanding of the strong interaction and discriminate between alternative descriptions. This possibility has motivated the analysis performed in this paper, where we have presented, for the first time, a comprehensive study of the single inclusive jet photoproduction at very forward rapidities in pp and pPb collisions at LHC energies using the Color Dipole formalism. Such process can, in principle, be separated considering that the hadron that act as source of photons will remain intact and a rapidity gap associated to the photon exchange will be present in the final state. We have focused in the rapidity range probed by the CMS-CASTOR calorimeter, which implies that the QCD dynamics is probed at very small values of x ($\leq 10^{-5}$), where the contribution of the non-linear effects is expected to be non-negligible. In our analysis we have estimated the cross sections using the IP-SAT, IP-NONSAT and bCGC models, which taken into account the non-linear effects and are able to describe the very precise ep HERA data. As the free parameters present in the Color Dipole formalism have been constrained by the HERA data, the predictions for LHC energies are parameter free. We have presented our predictions for the transverse momentum and energy spectrum and demonstrated that these distributions are sensitive to the phenomenological model used to describe the QCD dynamics. Therefore, a future experimental analysis of the single jet photoproduction can be useful to probe the Color Dipole formalism and the underlying assumptions present in the description of the linear and non-linear regimes of the QCD dynamics.

Acknowledgements VPG acknowledges useful discussions with C. Royon about the CMS-CASTOR calorimeter during your visit to the Department of Physics and Astronomy of the University of Kansas and would like to express a special thanks to the Mainz Institute for Theoretical Physics (MITP) of the Cluster of Excellence PRISMA+ (Project ID 39083149) for its hospitality and support. This work was partially financed by the Brazilian funding agencies CAPES, CNPq, FAPERGS and INCT-FNA (process number 464898/2014-5).

Data Availability Statement This manuscript has no associated data or the data will not be deposited. [Authors' comment: This is a theoretical research work, so no additional data is associated with the article.]

Funded by SCOAP[3].

References

1. Y. Dokshitzer, Sov. Phys. JETP **46**, 641 (1977)
2. V.N. Gribov, L.N. Lipatov, Sov. J. Nucl. Phys. **15**, 438 (1972)
3. G. Altarelli, G. Parisi, Nucl. Phys. B **126**, 298 (1977)
4. L.V. Gribov, E.M. Levin, M.G. Ryskin, Phys. Rept. **100**, 1 (1983)
5. F. Gelis, E. Iancu, J. Jalilian-Marian, R. Venugopalan, Ann. Rev. Nucl. Part. Sci. **60**, 463 (2010)
6. H. Weigert, Prog. Part. Nucl. Phys. **55**, 461 (2005)
7. J. Jalilian-Marian, Y.V. Kovchegov, Prog. Part. Nucl. Phys. **56**, 104 (2006)
8. A. Deshpande, R. Milner, R. Venugopalan, W. Vogelsang, Ann. Rev. Nucl. Part. Sci. **55**, 165 (2005)
9. D. Boer, M. Diehl, R. Milner, R. Venugopalan, W. Vogelsang, D. Kaplan, H. Montgomery and S. Vigdor et al., arXiv:1108.1713 [nucl-th]
10. A. Accardi, J.L. Albacete, M. Anselmino, N. Armesto, E.C. Aschenauer, A. Bacchetta, D. Boer, W. Brooks et al., Eur. Phys. J. A **52**(9), 268 (2016)
11. E.C. Aschenauer et al., Rept. Prog. Phys. **82**(2), 024301 (2019)
12. K. Akiba et al., LHC Forward Physics Working Group Collaboration. J. Phys. G **43**, 110201 (2016)
13. J.L. Albacete, C. Marquet, Prog. Part. Nucl. Phys. **76**, 1 (2014)
14. I.I. Balitsky, Nucl. Phys. B **463**, 99 (1996)
15. I.I. Balitsky, Phys. Rev. Lett. **81**, 2024 (1998)
16. I.I. Balitsky, Phys. Rev. D **60**, 014020 (1999)
17. I.I. Balitsky, Phys. Lett. B **518**, 235 (2001)
18. Y.V. Kovchegov, Phys. Rev. D **60**, 034008 (1999)
19. Y.V. Kovchegov, Phys. Rev. D **61**, 074018 (2000)
20. J. Jalilian-Marian, A. Kovner, L. McLerran, H. Weigert, Phys. Rev. D **55**, 5414 (1997)
21. J. Jalilian-Marian, A. Kovner, H. Weigert, Phys. Rev. D **59**, 014014 (1999)
22. J. Jalilian-Marian, A. Kovner, H. Weigert, Phys. Rev. D **59**, 014015 (1999)
23. J. Jalilian-Marian, A. Kovner, H. Weigert, Phys. Rev. D **59**, 034007 (1999)
24. E. Iancu, A. Leonidov, L. McLerran, Nucl. Phys. A **692**, 583 (2001)
25. E. Ferreiro, E. Iancu, A. Leonidov, L. McLerran, Nucl. Phys. A **701**, 489 (2002)
26. H. Weigert, Nucl. Phys. A **703**, 823 (2002)
27. F.O. Duraes, A.V. Giannini, V.P. Goncalves, F.S. Navarra, Phys. Rev. C **94**(2), 024917 (2016)
28. B. Ducloue, T. Lappi, Y. Zhu, Phys. Rev. D **93**(11), 114016 (2016)
29. B. Ducloue, T. Lappi, Y. Zhu, Phys. Rev. D **95**(11), 114007 (2017)
30. K. Kutak, H. Van Haevermaet, P. Van Mechelen, Phys. Lett. B **770**, 412 (2017)
31. M. Bury, H. Van Haevermaet, A. Van Hameren, P. Van Mechelen, K. Kutak, M. Serino, Phys. Lett. B **780**, 185 (2018)
32. H. Mantysaari, H. Paukkunen, Phys. Rev. D **100**(11), 114029 (2019)
33. A.M. Sirunyan et al., CMS Collaboration, JHEP **1905**, 043 (2019)
34. C.A. Bertulani, G. Baur, Phys. Rep. **163**, 299 (1988)
35. F. Krauss, M. Greiner, G. Soff, Prog. Part. Nucl. Phys. **39**, 503 (1997)
36. G. Baur, K. Hencken, D. Trautmann, J. Phys. G **24**, 1657 (1998)
37. G. Baur, K. Hencken, D. Trautmann, S. Sadovsky, Y. Kharlov, Phys. Rep. **364**, 359 (2002)
38. C.A. Bertulani, S.R. Klein, J. Nystrand, Ann. Rev. Nucl. Part. Sci. **55**, 271 (2005)
39. V.P. Goncalves, M.V.T. Machado, J. Phys. G **32**, 295 (2006)
40. A.J. Baltz et al., Phys. Rept. **458**, 1 (2008)
41. J.G. Contreras, J.D. Tapia Takaki, Int. J. Mod. Phys. A **30**, 1542012 (2015)
42. E. Basso, V.P. Goncalves, A.K. Kohara, M.S. Rangel, Eur. Phys. J. C **77**(9), 600 (2017)
43. N.N. Nikolaev, B.G. Zakharov, Phys. Lett. B **332**, 184 (1994)
44. N.N. Nikolaev, B.G. Zakharov, Z. Phys. C **64**, 631 (1994)
45. V.P. Goncalves, C.A. Bertulani, Phys. Rev. C **65**, 054905 (2002)
46. V.P. Goncalves, M.V.T. Machado, Eur. Phys. J. C **40**, 519 (2005)
47. S.R. Klein, J. Nystrand, Phys. Rev. C **60**, 014903 (1999)
48. L. Frankfurt, M. Strikman, M. Zhalov, Phys. Lett. B **540**, 220 (2002)
49. S.R. Klein, J. Nystrand, Phys. Rev. Lett. **92**, 142003 (2004)
50. V.P. Goncalves, M.V.T. Machado, Phys. Rev. C **73**, 044902 (2006)
51. V.P. Goncalves, M.V.T. Machado, Phys. Rev. D **77**, 014037 (2008)
52. V.P. Goncalves, M.V.T. Machado, Phys. Rev. C **80**, 054901 (2009)
53. L. Frankfurt, M. Strikman, M. Zhalov, Phys. Lett. B **537**, 51 (2002)
54. L. Frankfurt, M. Strikman, M. Zhalov, Phys. Rev. C **67**, 034901 (2003)
55. L. Frankfurt, V. Guzey, M. Strikman, M. Zhalov, JHEP **0308**, 043 (2003)
56. W. Schafer, A. Szczurek, Phys. Rev. D **76**, 094014 (2007)
57. A. Rybarska, W. Schafer, A. Szczurek, Phys. Lett. B **668**, 126 (2008)
58. A. Cisek, W. Schafer, A. Szczurek, Phys. Rev. C **86**, 014905 (2012)
59. V.P. Goncalves, M.V.T. Machado, Phys. Rev. C **84**, 011902 (2011)
60. A.L. Ayala Filho, V.P. Goncalves, M.T. Griep, Phys. Rev. C **78**, 044904 (2008)
61. A. Adeluyi, C. Bertulani, Phys. Rev. C **84**, 024916 (2011)
62. A. Adeluyi, C. Bertulani, Phys. Rev. C **85**, 044904 (2012)
63. L. Motyka, G. Watt, Phys. Rev. D **78**, 014023 (2008)
64. T. Lappi, H. Mantysaari, Phys. Rev. C **87**, 032201 (2013)
65. M.B. Gay Ducati, M.T. Griep, M.V.T. Machado, Phys. Rev. D **88**, 017504 (2013)
66. M.B. Gay Ducati, M.T. Griep, M.V.T. Machado, Phys. Rev. C **88**, 014910 (2013)
67. V. Guzey, M. Zhalov, JHEP **1310**, 207 (2013)
68. V. Guzey, M. Zhalov, JHEP **1402**, 046 (2014)
69. S.P. Jones, A.D. Martin, M.G. Ryskin, T. Teubner, JHEP **1311**, 085 (2013)
70. G. Sampaio dos Santos, M.V.T. Machado, Phys. Rev. C **89**, 025201 (2014)
71. G. Sampaio dos Santos, M.V.T. Machado, Phys. Rev. C **91**, 025203 (2015)
72. V.P. Goncalves, B.D. Moreira, F.S. Navarra, Phys. Rev. C **90**, 015203 (2014)
73. V.P. Goncalves, B.D. Moreira, F.S. Navarra, Phys. Lett. B **742**, 172 (2015)
74. Y.P. Xie, X. Chen, Eur. Phys. J. C **76**(6), 316 (2016)
75. Y.P. Xie, X. Chen, Nucl. Phys. A **959**, 56 (2017)
76. V.P. Goncalves, B.D. Moreira, F.S. Navarra, Phys. Rev. D **95**, 054011 (2017)
77. V.P. Goncalves, F.S. Navarra, D. Spiering, Phys. Lett. B **768**, 299 (2017)
78. V.P. Goncalves, F.S. Navarra, D. Spiering, Phys. Lett. B **791**, 299 (2019)
79. G. Chen, Y. Li, P. Maris, K. Tuchin, J.P. Vary, Phys. Lett. B **769**, 477 (2017)
80. V.P. Goncalves, M.V.T. Machado, B.D. Moreira, F.S. Navarra, G.S.D. Santos, Phys. Rev. D **96**(9), 094027 (2017)
81. S.R. Klein, J. Nystrand, R. Vogt, Eur. Phys. J. C **21**, 563 (2001)
82. S.R. Klein, J. Nystrand, R. Vogt, Phys. Rev. C **66**, 044906 (2002)
83. V.P. Goncalves, M.V.T. Machado, Eur. Phys. J. C **31**, 371 (2003)
84. V.P. Goncalves, M.V.T. Machado, Phys. Rev. D **71**, 014025 (2005)
85. V.P. Goncalves, M.V.T. Machado, A.R. Meneses, Phys. Rev. D **80**, 034021 (2009)
86. V.P. Goncalves, Phys. Rev. D **88**(5), 054025 (2013)
87. R. Vogt, hep-ph/0407298

88. M. Strikman, R. Vogt, S.N. White, Phys. Rev. Lett. **96**, 082001 (2006)
89. V.P. Goncalves, C. Potterat, M.S. Rangel, Phys. Rev. D **93**(3), 034038 (2016)
90. P. Kotko, K. Kutak, S. Sapeta, A.M. Stasto, M. Strikman, Eur. Phys. J. C **77**(5), 353 (2017)
91. V.P. Goncalves, G. Sampaio dos Santos, C.R. Sena, Nucl. Phys. A **976**, 33 (2018)
92. V. Guzey, M. Klasen, Phys. Rev. C **99**(6), 065202 (2019)
93. V. Guzey, M. Klasen, Eur. Phys. J. C **79**(5), 396 (2019)
94. The ATLAS collaboration [ATLAS Collaboration], ATLAS-CONF-2017-011
95. V.M. Budnev, I.F. Ginzburg, G.V. Meledin, V.G. Serbo, Phys. Rept. **15**, 181 (1975)
96. M. Drees, D. Zeppenfeld, Phys. Rev. D **39**, 2536 (1989)
97. N.N. Nikolaev, W. Schafer, Phys. Rev. D **71**, 014023 (2005)
98. B. Floter, B.Z. Kopeliovich, H.J. Pirner, J. Raufeisen, Phys. Rev. D **76**, 014009 (2007)
99. H. Kowalski, L. Motyka, G. Watt, Phys. Rev. D **74**, 074016 (2006)
100. A.H. Rezaeian, I. Schmidt, Phys. Rev. D **88**, 074016 (2013)
101. E. Levin, K. Tuchin, Nucl. Phys. A **691**, 779 (2001)
102. H. Kowalski, D. Teaney, Phys. Rev. D **68**, 114005 (2003)
103. H. Kowalski, T. Lappi, R. Venugopalan, Phys. Rev. Lett. **100**, 022303 (2008)
104. H. Mantysaari, P. Zurita, Phys. Rev. D **98**, 036002 (2018)
105. K.J. Golec-Biernat, M. Wusthoff, Phys. Rev. D **59**, 014017 (1998)